



Ionic Compatibilization of polypropylene/polyamide 6 blends using an ionic liquids/nanotalc fillers combination: morphology, thermal and mechanical properties

Journal:	<i>RSC Advances</i>
Manuscript ID:	RA-ART-01-2015-000816.R1
Article Type:	Paper
Date Submitted by the Author:	14-May-2015
Complete List of Authors:	Yousfi, Mohamed; ecole des mines, Livi, Sébastien; Cornell University, MS&E dumas, angel; University of Toulouse, Crepin-leblond, Jerome; Imerys, Greenhillhooper, Mike; Imerys, Duchat, Jannick; INSA de Lyon, IMP

ARTICLE

Ionic Compatibilization of polypropylene/polyamide 6 blends using an ionic liquids/nanotalc fillers combination: morphology, thermal and mechanical properties

Cite this: DOI: 10.1039/x0xx00000x

Received 00th January 2012,
Accepted 00th January 2012

DOI: 10.1039/x0xx00000x

www.rsc.org/

M. Yousfi^a, S. Livi^a, A. Dumas^b, J. Crépin-Leblond^c, M. Greenhill-Hooper^c
and J. Duchet-Rumeau^a

In this study, room temperature ionic liquids (RTILs) based on phosphonium cations have been used as effective compatibilizers of polyolefin/polyamide 6/synthetic talc blends using a melt extrusion process. Thus, different ionic liquids functionalized by various counteranions (phosphinate versus bistriflimide) were introduced at various concentrations (1, 5 and 10 wt%) in the polymer mixtures. Then, the crystallization behaviour, the thermal and mechanical properties of blends as well as the morphologies were investigated. The transmission electronic microscopy (TEM) micrographs demonstrated that the use of a very low of ILs (1wt%) led to a significant reduction of the size of the dispersed PA 6 phase. Moreover, the thermal properties of PP/PA6/talc was dramatically enhanced (+80 °C) and the mechanical performance was improved without reducing the strain at break suggesting a synergistic effect between nanotalc and ionic liquids.

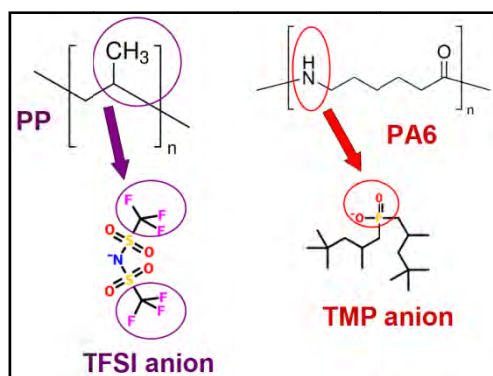
A Introduction

The development of polymer blend based materials has attracted great interest over the past several decades and is currently considered as a very active area of science and technology of great economic importance¹. Blending two or more polymers is a suitable route for producing new engineering polymers at low cost and desirable properties combination for specific end use. They can be developed much more quickly than new synthetic polymers and require much less capital investment². Unfortunately, most pairs of polymers are not compatible with each other from a thermodynamic point of view. These immiscible blends are characterized by a two phase morphology, poor physical and chemical interactions across the phase boundaries, and poor mechanical properties which had limited their use in industry³. A compatibilizing method is required to achieve a good interfacial adhesion between the two immiscible components⁴. Typical examples of immiscible polymer blends are blends of polypropylene (PP) and polyamide (PA6). PP and PA6 are among the most widely used plastics in the world. They represent two important classes of polymers with complementary properties. For blends

containing a PA6-rich phase, the polypropylene was added because it provides mainly high dimensional stability especially in humidity which improves the impact resistance of polyamide. On the other hand, for PP-rich blends, the main incentives to added polyamide have been the need to improve the heat resistance and tensile properties of polypropylene. To that end, research activities concerning the compatibilization of polypropylene and polyamide 6 date back to 1974, when Ide and Hasegawa⁵ used maleic anhydride grafted PP (PPgMA) as a compatibilizer to enhance the miscibility between PP and PA6. This coupling agent is still one of the most widely used compatibilizers in these blends. However, PPgMA must be added within a large amount (10 – 20 wt% minimum) to achieve the desired properties leading to an increase in the price of the final product. Recently, mechanochemistry of polymers in the solid state was used as a new strategy of compatibilization of immiscible polymer blends⁶. Unmelted polymers are subjected to intense shearing action and interpolymer radical reactions during solid-state shear extrusion pulverization process was observed⁷. Unfortunately, the most of the compatibilizing methods previously cited induces a significant loss of blend stiffness. Nanoparticles, especially

organically modified clays (organoclays), have attracted a great interest since the nanofiller is usually inexpensive, and can play the role of a structural reinforcement and a compatibilizer for many immiscible polymer blends. Researchers have proposed several explanations on the compatibilizing effect of organoclay on immiscible polymer blends depending on the affinity of the filler with each component of the blend. Unfortunately, the most of the commercially available organoclays used for the compatibilization of polymer blends are not thermally stable and their organo-modifiers are degraded easily when used as interfacial agents for engineering polymers such as (PA6, PET, PC) requiring a high temperature of processing leading to not satisfactory properties⁸⁻¹⁰. To overcome these limitations, ionic liquids (*i.e.* organic salts that keep the liquid state even at room temperature) appear as new promising stable surfactants. Due to their thermal stability, their non-combustibility, their low volatility and other specific properties, imidazolium and phosphonium ionic liquids have been widely used as modifier agents of layered silicates leading to a better dispersion of clay in the polymer matrix generally coupled with an enhancement of the final properties of materials¹¹. Despite all the benefits of ionic liquids previously cited, few works have been investigated on the application of ionic liquids in the compatibilization of polymer blends. Therefore, our approach is to present the ability of using ionic liquids (ILs) to act as effective compatibilizers within polyolefin/polyamide blends. The combination of ionic liquids and nanotalc in the blends was an attempt made to reach a balance between ductility and strength properties. The synergistic effect induced by the simultaneous presence of ionic liquids and talc on morphology, crystallization, thermal and mechanical properties of blends was studied.

Two kinds of ionic liquids were used: an hydrophobic and an hydrophilic one. The role of the counter anion in the ionic liquid was highlighted since ILs contain the same phosphonium cation but differ by the polarity of their anions. The anions selected have a special affinity with PP matrix in the case of trifluoromethyl sulfonylimide (TFSI) or PA6 phase in the case of trimethylpentyl phosphinate (TMP) (Scheme1).



Scheme 1. Degree of compatibility between the ionic liquids (anion) and each polymer.

B Experimental

B.1 Materials

Polypropylene HP500N (density 0.9 g/cm³, melt flow index 12 g/10 min [230 °C, 2.16 kg], melting temperature 167 °C) was supplied by LyondellBasell (France). Polyamide 6 (PA6) under commercial name Technyl S-27 BL (density 1.13 g/cm³, melting temperature 222 °C) was produced by Solvay (France). Synthetic nanotalc was provided by the GET Laboratory (Toulouse University, France). Thereafter, the abbreviation HT will be attributed to the synthetic talc. The ionic liquids (ILs) kindly supplied by Cytec were trihexyl(tetradecyl)phosphonium bis(2,4,4-trimethylpentyl)phosphinate (molar mass = 773 g.mol⁻¹) and (trihexyl)tetradecylphosphonium bis(trifluoromethylsulfonyl)imide (molar mass = 764 g.mol⁻¹) denoted as IL-TMP and IL-TFSI, respectively. The structures and nomenclatures of phosphonium ionic liquids are presented in Table 1.

Table 1. Designation of ionic liquids used.

Commercial name	Designation	Cation structure	Anion structure
CYPHOS® IL104	IL-TMP		
CYPHOS® IL109	IL-TFSI		

B.2 Synthesis of talc

Nanometric talcs were synthesized at GET Laboratory (Toulouse University, France) according to a hydrothermal process developed by Martin *et al.*¹². The synthetic talc with a specific surface area of 131 m².g⁻¹, equivalent to the 6H-talc sample studied by Dumas *et al.*¹³, was used as a gel (output of the synthesis reactor). After the preparation of a talc precursor at room temperature that respect the Mg/Si talc ratio, an hydrothermal treatment of 6 hours was used to obtain the crystalline nanotalc.

B.3 Processing and characterization of the polymer blends

Before extrusion, PA6 pellets were dried in a vacuum oven overnight at 80 °C.

Nanocomposites based on PP/PA6, PP/PA6/talc without and with ILs were prepared under nitrogen atmosphere using a 15 g-capacity DSM micro-extruder (Midi 2000 Heerlen, The Netherlands) with co-rotating screws. The mixture was sheared for about 10 min with a 240 rpm speed at 240 °C and injected in a 10 cm³ mould at 80 °C to obtain disk and dumbbell-shaped specimens. All the compositions of the polymer blends are presented in Table 2.

Table 2: Composition of the blends used

Sample	Designation	m(PP):m(PA6):m(talc):m(IL)
B0	PP:PA6	80:20:0:0
B1	PP:PA6:HT:IL-TMP-1%	80:20:0:1
B2	PP:PA6:HT:IL-TMP-2%	80:20:0:2
B3	PP:PA6:HT:IL-TMP-5%	80:20:0:5
B4	PP:PA6:HT:IL-TMP-10%	80:20:0:10
B5	PP:PA6:HT:IL-TFSI-1%	80:20:0:1
B6	PP:PA6:HT:IL-TFSI-5%	80:20:0:5

Surface energy of talc was determined with the sessile drop method on a GBX goniometer. From contact angle measurements with water and diiodomethane as test liquids on pressed modified talc disks, polar and dispersive components of surface energy were determined using the Owens–Wendt theory¹⁴.

Thermogravimetric analyses (TGA) of composites were performed on a Q500 thermogravimetric analyzer (TA instruments). The samples were heated from 30 to 700 °C at a rate of 20 K min⁻¹ under air flow.

Transmission electron microscopy (TEM) was carried out at the Technical Center of Microstructures (University of Lyon) on a Phillips CM 120 microscope operating at 80 kV to characterize the level of dispersion of talc particles in the matrix. The samples were cut using an ultramicrotome equipped with a diamond knife, to obtain 60-nm-thick ultrathin sections. Then, the sections were set on copper grids. ImageJ Software (U.S. National Institutes of Health) was used to estimate the mean diameter of particles in each sample.

DSC measurements were carried out by using Q20 (TA instruments) in the range of 10 °C to 270 °C. The samples were kept for 3 min at 270 °C to erase the thermal history before being heated or cooled at a rate of 10 K min⁻¹ under nitrogen flow of 50 mL/min. The melting temperature (T_m) and crystallization temperature (T_c) of PP and PA6 phases, are determined as the maximum of melting and crystallization peak from second heating and cooling DSC thermograms respectively. $t^{1/2}$ represents the time corresponding to 50% of the relative crystallinity.

Uniaxial tensile measurements (elongation at break) were taken using a MTS 2/M electromechanical testing system at 22 ± 1 °C and $50 \pm 5\%$ relative humidity and were performed with a speed of 40 mm min⁻¹. Young's modulus measurements were taken by means of an extensometer using an Instron 4301 machine at a cross-head speed of 1 mm.min⁻¹. A minimum of five tensile specimens were tested for each reported value.

C Results and discussion

C.1 Surface energy of talc fillers and polymers

The contact angles and the surface energy determined by the sessile drop method on pressed talc powders and polymers are summarized in Table 3. To highlight the chemical affinity of ionic liquids with polymer matrices composing the blend, a drop of IL-TFSI and IL-TMP were deposited on the neat polypropylene and polyamide 6.

As the synthetic talc nanoparticles have a larger specific surface area, a higher surface energy is obtained¹⁵. Their surface tension is closer to polyamide 6 matrix one compared to PP matrix one, particularly the high polar components are similar. In both cases, ionic liquids have a surface energy close to the polypropylene matrix with values in the range of 30.7-30.4 mN/m for IL-TMP and IL-TFSI, respectively. These values are consistent with the literature where for example, different authors have also determined similar surface energies for these phosphonium salts^{16, 17}. However, significant differences were observed with the PP matrix. In fact, when a drop of ionic liquid denoted IL-TFSI is deposited on the polymer matrix, a contact angle of 38 ± 5 ° is obtained while for the ionic liquid named IL-TMP, a value of 54 ± 4 ° is observed. These results highlight the best wetting of IL-TFSI with polypropylene matrix, therefore the chemical nature of the counter anion plays a key role in the dispersion of the ionic liquid within polymer blends.

Table 3. Determination of total, polar, and dispersive components of the surface energy at 20 °C on PP, PA6, IL-TFSI, IL-TMP and contact angles values of ILs on polypropylene and polyamide 6.

Samples	Contact angle (°)	γ polar (mN/m)	γ dispersive (mN/m)	Surface energy (mN/m)
PP ¹⁸	-	0.4	28.6	29
PA6 ¹⁹	-	29.1	23.8	52.9
Talc	$\Theta_{H_2O}=34$ $\Theta_{CH_2I_2}=48$	29.6	35.1	64.7
IL-TFSI	-	-	-	30.4
IL-TMP	-	-	-	30.7
PP	$\Theta_{IL-TFSI}=38$ $\Theta_{IL-TMP}=54$			
PA6	$\Theta_{IL-TFSI}=42$ $\Theta_{IL-TMP}=41$			

C.2 Effect of ionic liquids on the morphology of PP/PA6/talc nanocomposites

In order to probe at a nanometric scale the influence of ILs on the morphology of talc filled PP/PA6 blends, the transmission electron microscopy have been performed. The distribution and dispersion of PA6 domains in polypropylene matrix but also the location of the talc layers (the dark lines) in the polymer blend are reported in Figures 1 and 2. It's useful to mention that despite the precautions and efforts to improve the preparation of samples, the elevated stiffness (hardness) of some PA6 nodules particularly for samples containing 1wt% of ILs, generates bright white spots which appear in their corresponding TEM images.

Due to the poor interactions at the molecular level and the relatively high interfacial tension between PP and PA6, a phase-separated morphology combined with a poor interfacial adhesion is generated spontaneously. In fact, a continuous PP phase with dispersed PA6 domains has been observed (Figure 1). Thus, using image analysis, PA6 phases had diameters in the range of $27.1 \pm 8.3 \mu\text{m}$. However, in all compatibilized blends, an homogeneous morphology consisting of nearly spherical PA6 droplets distributed homogeneously in a PP matrix can be observed (Figure 2).

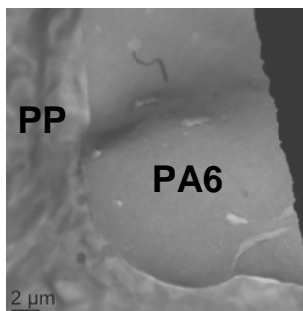


Figure 1: TEM images of virgin PP/PA6 blends.

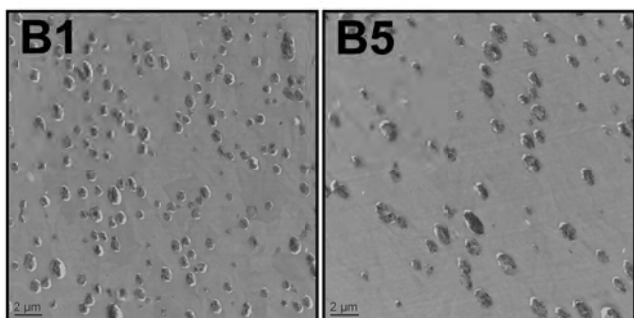


Figure 2: TEM images of PP/PA6/talc composites with 1%-IL-TMP (left) and 1% IL-TFSI (right).

Thus, the influence of the chemical nature of the anion (phosphinate versus sulfonamide *i.e.* IL-TMP versus IL-TFSI) has been studied on the morphologies of polymer blends. In all the cases, it was observed that talc is embedded within the PA6 phase or located at the matrix / droplet interface. In fact, the TEM images show a few to several talc platelets intercalated inside the PA6 droplets. These results confirm that synthetic talc has a much higher affinity for PA6 phase via strong polar-polar interactions. Indeed, since the PP/PA6 blend components have different surface tensions, hydrophilic talc particles are more inclined to be located in the most polar polymer phase having the higher surface tension (PA6) to minimize the interfacial tension. There are many data concerning this type of solid filler selective adsorption within one phase of the blend which confirms this point of view²⁰.

The decrease of the size of the dispersed phase due to the addition solely of talc nanoparticles has been reported recently in another paper²¹ and was attributed to the formation of a three-dimensional network of nanoparticles. According to the authors, the compatibilization effect was induced by the high delamination of nanotalc in the polyamide phase based on the encapsulation of PA6 domains in a three-dimensional network of nanoparticles. Thus, when the nanoparticles are well distributed inside the dispersed phase, they can form a three-dimensional network and the droplets

will be trapped in the array of nanoparticles. The mechanical stability of the network formed reduces the rate of coalescence leading to a significant reduction of the dispersed domain size from $27.1 \mu\text{m}$ to $2.8 \mu\text{m}$ in the case of the unfilled blends and nanocomposites respectively.

In a previous study²², our group highlighted that the addition of only 1 wt % of ILs into PP/PA6 blends induced to a significant decrease of the PA6 phases (from $27.1 \mu\text{m}$ to less than $3 \mu\text{m}$). In addition, the talc/ionic liquid combination induces a true synergistic effect. Indeed, with 1% of IL-TMP and 4% of talc, the diameter of the PA6 nodules decreases to $0.7 \mu\text{m} \pm 0.3 \mu\text{m}$ whereas with 1% of IL-TFSI and 4% of talc, the mean diameter is $0.9 \mu\text{m} \pm 0.6 \mu\text{m}$. This phenomenon is commonly encountered in polymer blends when nanoparticles²³, copolymers⁵ or ionomers³ are used. For example, Willis et al have demonstrated that the use of 5% of ionomer composed of 80% PE and 20% of methacrylic acid, partially neutralized with zinc in PP/PA6 (90/10) led to a decrease in the size of the PA6 phases from $2.7 \mu\text{m}$ to $1.1 \mu\text{m}$ ³. More recently, Fenouillot et al have also demonstrated that the use of nanoparticles in a polymer blends acts like an emulsifier which stabilize the mixture²⁴. Finally, talc nanoparticles might act as a solid barrier between the polymers because an accumulation of talc nanofillers at the interphase leads to a formation of a barrier around the minor phase which prevents the coalescence of PA6 domains leading to the formation of smaller particles²¹. In addition, a small amount of ionic liquid is enough to improve the compatibilization of PP/PA blends compared to the use of the copolymer such as maleated propylene (PPgMA) requiring an amount of 10-20 wt %^{25, 26}. When increasing the amount of ionic liquid in the polymer blends, a slight increase in the size of the PA6 phases is achieved. In particular, for 2% of ionic liquid introduced into the ternary mixture. In fact, the mean diameter in the presence of 2% of IL-TMP is about $1.6 \mu\text{m} \pm 1 \mu\text{m}$. In the opposite, the use of 5 wt% and 10 wt% of ionic liquid generated a novel decrease in the size of the drops of PA6 ($1.2 \mu\text{m}$ and $0.9 \mu\text{m}$ respectively).

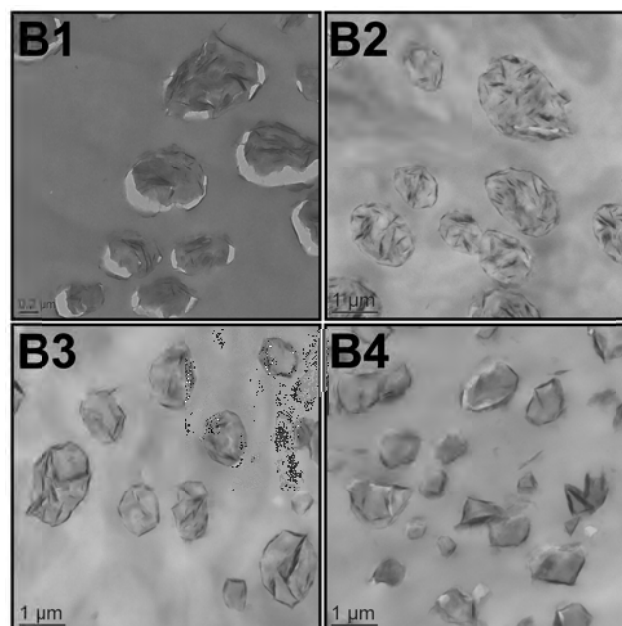


Figure 3: TEM micrographs illustrating the effect of ionic liquid content on the morphology: 1%- IL-TMP (B1), 2% IL-TMP (B2), 5%-IL-TMP (B3) and 10%-IL-TMP (B4).

In addition, a large amount of ionic liquid results in the formation of large talc tactoids randomly distributed in the PA6 nodules. Their size appears to be larger than in the presence of low ILs content. For PP/PA6 nanocomposites with 10% IL-TMP, a part of talc particles have migrated to the PP matrix. These results can be explained by the saturation induced by ionic liquids at the interface leading to a migration of talc tactoids outside of PA6 droplets. Filippone et al have observed similar phenomena in the case of PS/PMMA/OMMT blends²⁷. According to the authors, once the available interface is saturated, the exceeding particles are free to rearrange in the matrix. In the opposite, for high content of IL-TFSI (5 wt %), a surprising change in the morphology was obtained. Indeed, the shape and the size of PA6 domains were more heterogeneous: the form of particles were more elongated and oriented along the flow direction. Moreover, the talc persists as stack tactoids (agglomerates) inside the PA6 domains because of the low compatibility of the talc with the PA6 matrix. The mean diameter of fibrils was $0.6 \mu\text{m} \pm 0.3 \mu\text{m}$ and the length of the fibrils was $5.7 \pm 4.2 \mu\text{m}$.

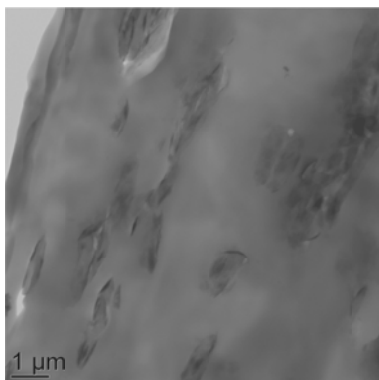


Figure 4: TEM images of PP/PA/talc composites with 5%-IL-TFSI.

C.3 Thermal properties of PP/PA6/talc/ionic liquids blends

The degradation mechanisms of nanocomposites have been investigated by thermogravimetric analysis (TGA). The onset temperature (T_{onset}) and the maximum degradation temperature (T_{max}) of the blends are presented in Table 4. The TGA curves and the corresponding derivative curves (DTG) of PP/PA6/talc without and with phosphonium ionic liquids are shown in Figures 5 and 6.

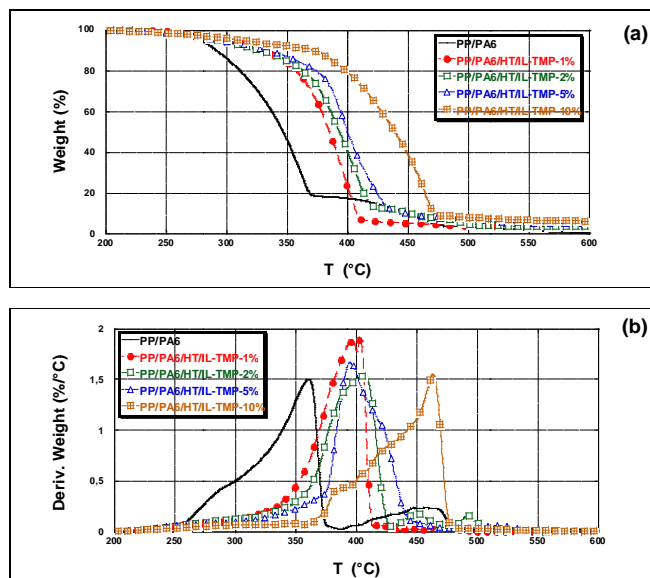


Figure 5: TGA (a) and DTG (b) curves of virgin and talc filled PP/PA6/IL-TMP composites.

Two populations have been clearly identified for PP/PA6 blends corresponding to the degradation of i) virgin polypropylene matrix at 360 °C and ii) virgin polyamide 6 at 457 °C. Then, when the ionic liquids are used, a significant decrease in thermal stability is observed. In addition, the amount of ionic liquid plays a key role in the degradation temperatures. Thus, 10 wt% of IL-TMP led to an increase in the onset of the thermal degradation process of 81 °C as well as an improvement in the degradation temperature of the PP phase (+ 102 °C) and in T_{max} of the PA6 (+ 46 °C) compared to PP/PA6 blend. In the case of PP/PA6/talc blends with 5% of phosphonium IL denoted IL-TFSI, an increase of the thermal stability of about 49 °C is achieved by comparison of the PP/PA6 blend (an increase of 48 °C and 66 °C in T_{max} were noted for PP matrix and PA6 phase, respectively). In a previous paper, we have studied the influence of talc fillers on the thermal stability of PP/PA6 blends and have found a significant enhancement of the thermal properties in the presence of nanotalc²¹. In fact, the dispersed talc particles induced a barrier which delayed the release of thermal degradation products in comparison with the pristine polymer blends. In another work on the influence of ILs on PP/PA6 blend, our group have demonstrated that the addition of ionic liquids led to a dramatic increase in the onset of decomposition of the virgin blends (+ 35 °C)²². In conclusion, the synergy created between the talc and the ionic liquid may explain the excellent thermal stability of the resulting nanocomposites.

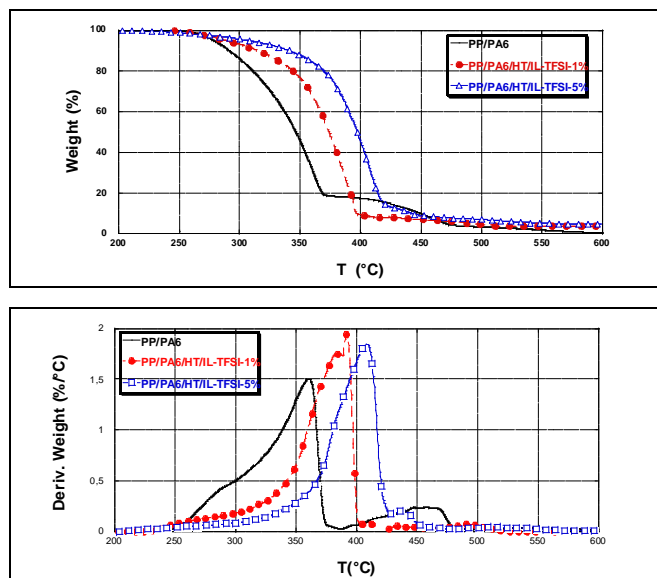


Figure 6: TGA (a) and DTG (b) curves of virgin and talc filled PP/PA6/IL-TFSI composites.

Table 4. TGA results of PP/PA6 blends and PP/PA6/HT/IL composites

Sample	$T_{\text{onset BLEND}} [^{\circ}\text{C}]$	$T_{\text{max PP}} [^{\circ}\text{C}]$	$T_{\text{max PA6}} [^{\circ}\text{C}]$
PP/PA6	291.7	360.3	456.8
PP/PA6/HT/IL-TMP-1%	330.8	402.0	471.6
PP/PA6/HT/IL-TMP-2%	328.4	405.5	492.5
PP/PA6/HT/IL-TMP-5%	335.8	395.5	517.4
PP/PA6/HT/IL-TMP-10%	373.1	462.7	502.4
PP/PA6/HT/IL-TFSI-1%	315.9	390.5	492.4
PP/PA6/HT/IL-TFSI-5%	340.8	408.0	522.4

C.4 Effect of ionic liquids on crystallisation behaviour of PP/PA6/talc/IL nanocomposites

The melting, crystallization temperatures and half crystallization time of virgin PP/PA6 binary blends and IL modified talc filled PP/PA6 nanocomposites are summarized in Table 5. The non-isothermal crystallization kinetic profile of PP phase with IL-TMP and IL-TFSI modified talc nanocomposites are presented in Figure 7. With the increase of IL amount in the polymer mixtures, it was observed that the curve reporting the relative crystallinity was shifted towards the longer times. In addition, the crystallization temperature (T_c) was shifted towards lower temperatures while increasing the IL content in the blends. The crystallization temperature (T_c) of PP was 122.1 °C for virgin PP/PA6 samples and decreased to 116.5 °C with weight ratio of 10wt% of IL-TMP. In the presence of IL-TFSI, T_c was lower (115.8°C) which highlights a better compatibility between PP and IL-TFSI compared to IL-TMP. The $t^{1/2}$ of PP component increased of about 30 seconds when the amount of IL-TMP and IL-TFSI reached 10wt% and 5wt% respectively in the blend indicating a slow-down crystallization process of PP component in the presence of ionic liquids. This phenomenon is known in the literature: In fact, Yang et al. have demonstrated that the crystallization time of PP in PP/PA6 blends compatibilized with PP-g-MA was longer than that of

uncompatibilized PP/PA6 blends²⁸. Thus, PP-g-PA6 generated by the chemical reaction between the functional group of PP-g-MA and the terminal groups of PA6 restricted the crystallization of PP. The same behavior have been highlighted by Xue et al on PP-g-MA compatibilized poly(trimethylene terephthalate)/polypropylene blends²⁹. The crystallization temperatures (T_c) of PTT and PP was shifted significantly to lower temperatures. The shift of PTT's (T_c) was higher than that of the PP, suggesting that addition of the PP-g-MA had a more significant effect on PTT crystallization than on PP due to reaction between maleic anhydride and PTT.

In this work, the crystallization temperatures of both PP and PA6 phases decreased with increasing ionic liquid content in the blends. This phenomenon highlights a slower crystallization rate of PP and PA6 domains.

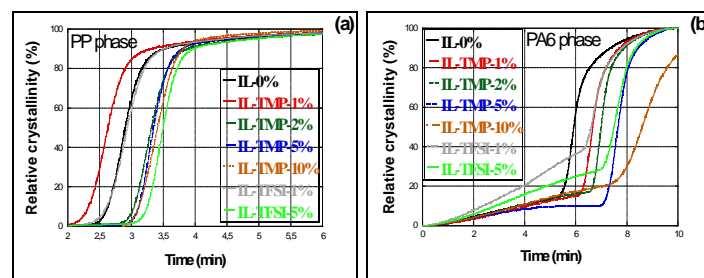


Figure 7: The relative crystallinity kinetics with crystallization time of PP phase (a) and PA6 phase (b) in PP/PA6 blends and PP/PA6/talc/ILs composites at different contents of ionic liquids.

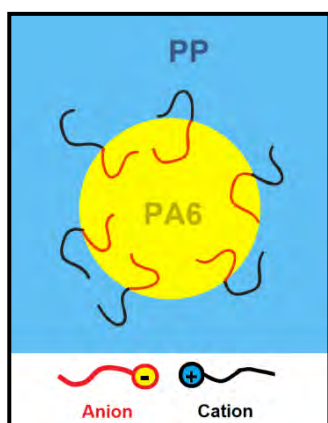
Figure 7(b) shows the non-isothermal crystallization rate of PA6 component for blends prepared in the presence of IL-TMP and IL-TFSI respectively. The crystallization process of PA6 was also delayed after the addition of ionic liquids. The (T_c) of PA6 phase decreased gradually with the increase of IL amounts and this decrease was more pronounced for the PA6 component compared to PP matrix. Indeed, T_c of PA6 was reduced to 165.3 °C (-26.5 °C) when the IL-TMP concentration in the blends increased to 10 wt % while the (T_c) of the PP phase was shifted only to 116.5 °C (-5.6 °C). According to the literature, Psarski et al. explained the slowing of the kinetics of crystallization of PA6 phase in PP/PA6 blends by the reduction of size of PA6 dispersed particles, caused by the interactions between the functional groups of the compatibilizer (PE-AA copolymer) and the polar groups in polyamide chain³⁰. By increasing the number of droplets per unit volume by decreasing the droplet size, the fraction of droplets that crystallizes at lower temperatures increases. But, this high shift cannot be explained only by the size of the PA6 domains.

In PP/PA6 blends, two distinct melting peaks are observed at 164.0 and 221.9 °C, corresponding to that of pure PP component and PA6 component, respectively. The (T_m) of PP in IL modified talc filled PP/PA6 composites show no significant shift compared with that of PP/PA6 blends. However, the (T_m) of PA6 in composites varies with the composition in comparison with the binary blend. When the IL-TMP was added for about 1 wt %, the (T_m) of PA6 was reduced by 3.6 °C, and the (T_m) of PP had no significant shifts (+0.9 °C). By increasing ILs concentration in the blends, the (T_m) of PA6

decreased much more and the shifts in 5 wt% IL-TMP and 10 wt% IL-TMP were 5.4 and 6 °C respectively.

Lahor et al. investigated sodium-neutralized poly(ethylene-co-methacrylic acid) ionomer to compatibilize PE-PA6 blends (80/20) at different concentrations³¹. They have demonstrated that the blends exhibited different crystallization and melting behaviours due to different content of ionomer. Since the ionomer has the ability to form interactions with both blend components, the (T_c) and (T_m) of PE and PA6 decreased after addition of the ionomer. This decrease was more pronounced when the weight ratio of ionomer increased.

In our case, the (T_m) and (T_c) shifts suggest that the compatibilization in PP/PA6 blends is achieved thanks to the ILs-nanotalc combination which promotes miscibility through mutual intermolecular interaction between nanotalc, IL-TMP or IL-TFSI and PP/PA6 phases. In fact, ILs acts as a real compatibilizer localized at the interface of PP/PA6 by establishing two kinds of interactions: i) polar – polar interactions could be formed between the polar groups beared by anion (sulfonamide for TFSI and phosphinate for TMP) and the amine groups. The level of these interactions will depend on the level of the polarity of each anion. ii) non polar – non polar interactions between the dispersive groups beared by the IL cation (aliphatic chains beared by phosphonium cation of ILs) and the non-polar units [—CH(CH₃)—] of PP. These two kinds of interactions can promote the interfacial miscibility between PP and PA6 phases (Scheme 2).



Scheme 2: Illustration of the mechanism of compatibilization of PP/PA6 blends by ionic liquids.

Table 5: The corresponding crystallization and melting parameters for virgin PP/PA6 blends and PP/PA6/talc/ILs composites with different contents of ionic liquids.

Sample	T_c (PP) (°C)	T_c PA6 (°C)	$t^{1/2}$ (PP) (min)	$t^{1/2}$ (PA6) (min)	T_m (PP) (°C)	T_m (PA6) (°C)
PP/PA6	122.1	191.8	2.94	5.95	164.0	221.9
PP/PA6/HT/IL-TMP-1%	124.5	184.2	2.67	6.69	164.9	218.3
PP/PA6/HT/IL-TMP-2%	118.0	180.6	3.35	7.02	165.6	218.1
PP/PA6/HT/IL-TMP-5%	117.9	174.3	3.39	7.68	164.0	216.5
PP/PA6/HT/IL-TMP-10%	116.5	165.3	3.45	8.63	165.2	215.9
PP/PA6/HT/IL-TFSI-1%	121.4	183.0	2.98	6.63	164.9	217.9
PP/PA6/HT/IL-TFSI-5%	115.8	174.7	3.54	7.52	164.2	217.2

C.5 Mechanical properties of PP/PA6/Talc/Ionic liquids nanocomposites

The mechanical properties *i.e.* the moduli and the fracture properties of the PP/PA6 blends and PP/PA6/Talc with IL-TMP and IL-TFSI are detailed in Figures 8 and 9. In addition, the tensile yield strengths for the different compositions are summarized in Table 6.

In all cases, the use of ILs denoted IL-TFSI and IL-TMP led to an increase of the Young Modulus. In particular, the greatest improvements are obtained for 1 wt% of phosphonium ILs. However, the chemical nature of the counter anion plays a key role: Indeed, 1 wt% of IL-TMP induced an increase of the Young Modulus of 37.6 % ($E = 1.88$ GPa for the PP/PA6 blends and 2.59 GPa with 1%-IL-TMP) whereas IL-TFSI led to an increase of 21.5 %. This result can be explained by the poor dispersion of nanotalc inside the PA6 nodules in the presence of IL-TFSI surfactants where the ionic interactions are less favourable (Figure 4). When the amount of ILs increases, the stiffness of materials tends to decrease. For 10% IL-TMP and 5% IL-TFSI, the Young modulus was 25.7% and 21.5% lower compared to the PP/PA6 blend indicating that the excess of ionic liquid weakened the reinforcing effect. In a previous study, similar behaviour was already observed. Indeed, for PP/PA6 blends filled only with high amount of IL-TFSI and IL-TMP, a plasticizing effect was obtained²². In the opposite, compared to the virgin blend, the standard deviation of Young modulus increased for the blends containing ionic liquids probably due to the heterogeneity in the samples prepared on the mini-molding setup. It's interesting to note that the trend of the Young's modulus in the PP/PA6/talc/ILs composites depending on the kind of ionic liquid used looks like PP/PA6/talc ternary systems previously studied²¹ for which the highest elastic modulus was measured on PP/PA6/talc nanocomposites containing the more hydrophilic nanofiller. The strong interactions and the high quality of dispersion (exfoliation) of nanotalc layers inside the PA6 minor phase is thought to be mainly responsible for the enhanced mechanical properties^{32, 33}.

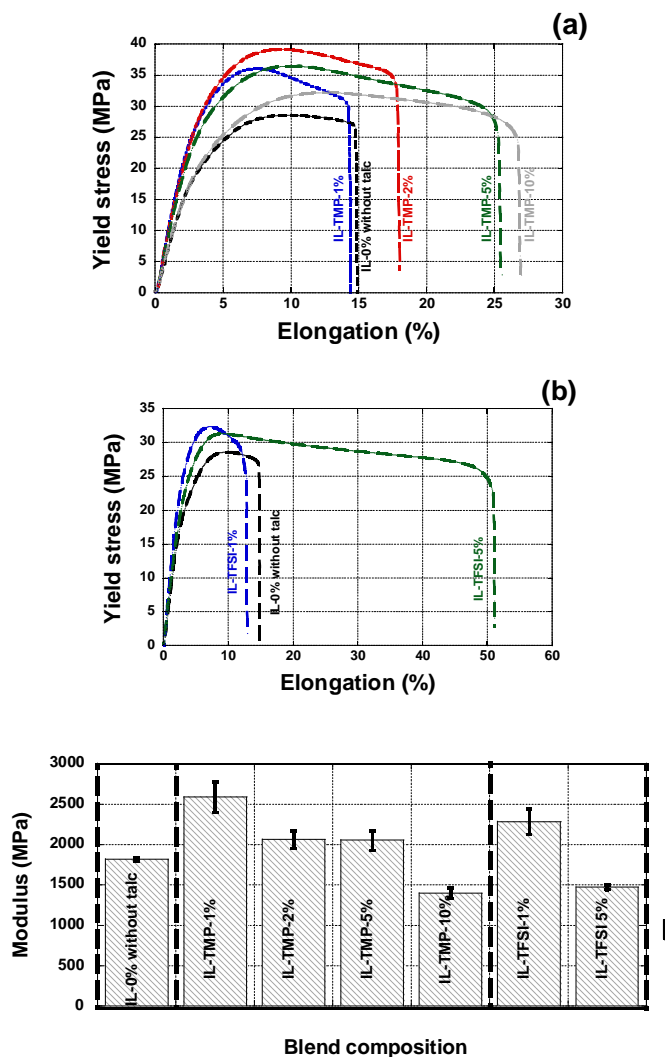


Figure 8: Stress–strain tensile curves and evolution of Young modulus as a function of the IL content within PP/PA6/talc nanocomposites. The PP/PA6 blend is given as reference.

Concerning the elongation at break, the trend is reversed. Indeed, an increase of the amount of ILs led to an increase of the fracture properties. For 1% IL-TMP, the elongation at break was 14% slightly lower than the unfilled PP/PA6 blend (17%). Similar behaviours were observed by Kusmono *et al.*³⁴ who showed that the addition of an organoclay (montmorillonite-octadecylamine) as a compatibilizer for PP/PA6 blend led to an enhancement in the stiffness of the blend but also to a decrease in elongation at break due to the high exfoliation of sheets that restricts chain mobility. Using the same PP/PA6 (80/20) blends filled with nanosilica, Laoutid *et al.*³⁵ found that the nanofillers reduced the size of the dispersed domains but at the same time acted as stress concentrating particles which reduced the ductility of the PP matrix.

Then, the addition of higher amounts of IL gradually increases the ductility of the polymer blends (23% and 42% for 5% of IL-TMP and IL-TFSI, respectively).

Moreover, the combined use of phosphonium ionic liquids and talc leads to an increase of the tensile yield strengths. In conclusion, the IL-talc combination provides a significant increase in stiffness without reducing the elongation at break.

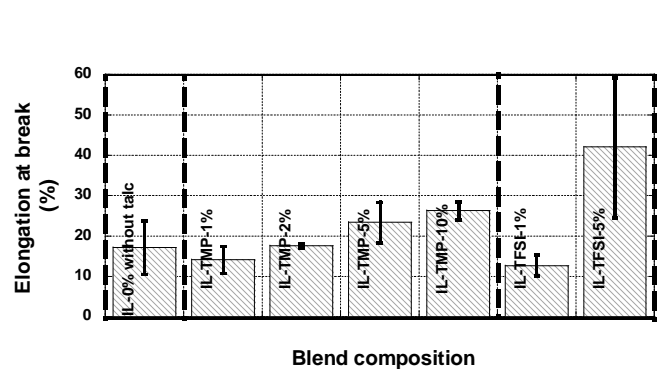


Figure 9: Evolution of the strain at break as a function of IL content within PP/PA6/Talc composites. The PP/PA6 blend is given as reference.

Table 6: The tensile yield strengths for virgin PP/PA6 blends and PP/PA6/talc/ILs composites with different contents of ionic liquids.

Sample	Yield stress (MPa)	Standard deviation (MPa)
IL-0% without talc	28.8	1.1
IL-TMP-1%	33.9	1.2
IL-TMP-2%	38.5	1.0
IL-TMP-5%	38.0	1.0
IL-TMP-10%	32.4	0.7
IL-TFSI-1%	32.6	0.7
IL-TFSI-10%	30.9	1.3

Conclusions

In this work, we have highlighted the good synergy between the nanotalc and the ionic liquids to improve the final properties of PP/PA6 blends. In fact, the incorporation of ionic liquid in PP/PA6/talc blends led to significant reductions in the size of the polyamide domains with a preferential localization of the talc in this matrix. In addition, substantial increases in the thermal stability (+ 60-80 °C) of the nanocomposites have been observed by using different amounts of ionic liquids denoted IL-TMP and IL-TFSI (1-5-10 wt%). Then, for mechanical properties, a reinforcing effect is obtained for a low amount of ionic liquid (1 wt%). In the opposite, when adding higher amount of ionic liquid, a plasticizing effect is observed causing a reduction in stiffness for the benefit of the deformation at break. In conclusion, phosphonium ionic liquids are excellent compatibilizing agents of binary or ternary thermoplastic blends mixtures and represent a real alternative to block copolymers or ionomer where large quantities are used^{22, 30-32}

Acknowledgement

This work was supported by financial funding from National Agency for Research (France) in the frame of the project “Nanotalc”. The authors acknowledge Dr Annie Rivoire and Dr Christelle Boule from Claude Bernard University for his help in microscopy experiments.

Notes and references

^a Université de Lyon, F-69003, Lyon, France; INSA Lyon, F-69621, Villeurbanne, France; CNRS, UMR 5223, Ingénierie des Matériaux Polymères.

^bUniversité de Toulouse, UPS, ERT Géomatériaux, F-31000 Toulouse, France, CNRS, UMR 5563, GET Géosciences Environnement Toulouse, ERT Géomatériaux, F-31400 Toulouse, France

^cImerys Talc, 2 Place E.-Bouillères 31036 Toulouse, France

1. C. W. Macosko, *Macromolecular Symposia*, 2000, **149**, 171-184.
2. E. Van Hemelrijck, P. Van Puyvelde, C. W. Macosko and P. Moldenaers, *Journal of Rheology*, 2005, **49**, 783-798.
3. J. M. Willis and B. D. Favis, *Polymer Engineering and Science*, 1988, **28**, 1416-1426.
4. J. C. Lepers, B. D. Favis and R. J. Tabar, *Journal of Polymer Science Part B-Polymer Physics*, 1997, **35**, 2271-2280.
5. F. Ide and A. Hasegawa, *Journal of Applied Polymer Science*, 1974, **18**, 963-974.
6. A. H. Lebovitz, K. Khait and J. M. Torkelson, *Polymer*, 2003, **44**, 199-206.
7. P. J. Brunner, J. T. Clark, J. M. Torkelson and K. Wakabayashi, *Polymer Engineering and Science*, 2012, **52**, 1555-1564.
8. W. H. Awad, J. W. Gilman, M. Nyden, R. H. Harris, T. E. Sutto, J. Callahan, P. C. Trulove, H. C. DeLong and D. M. Fox, *Thermochimica Acta*, 2004, **409**, 3-11.
9. M. Yousfi, J. Soulestin, B. Vergnes, M. F. Lacrampe and P. Krawczak, *Journal of Applied Polymer Science*, 2013, **128**, 2766-2778.
10. M. C. Costache, M. J. Heidecker, E. Manias, R. K. Gupta and C. A. Wilkie, *Polymer Degradation and Stability*, 2007, **92**, 1753-1762.
11. S. Livi, J. Duchet-Rumeau, P. Thi Nhan and J.-F. Gerard, *Journal of Colloid and Interface Science*, 2011, **354**, 555-562.
12. *France Pat.*, 2011.
13. A. Dumas, F. Martin, C. Le Roux, P. Micoud, S. Petit, E. Ferrage, J. Brendlé, O. Grauby and M. Greenhill-Hooper, *Physics and Chemistry of Minerals*, 2013, **40**, 361-373.
14. D. K. Owens and R. C. Wendt, *Journal of Applied Polymer Science*, 1969, **13**, 1741-1747.
15. M. Yousfi, S. Livi, A. Dumas, C. Le Roux, J. Crépin-Leblond, M. Greenhill-Hooper and J. Duchet-Rumeau, *Journal of Colloid and Interface Science*, 2013, **403**, 29-42.
16. H. F. D. Almeida, J. A. Lopes-da-Silva, M. G. Freire and J. A. P. Coutinho, *Journal of Chemical Thermodynamics*, 2013, **57**, 372-379.
17. P. J. Carvalho, C. M. S. S. Neves and J. A. P. Coutinho, *Journal of Chemical and Engineering Data*, 2010, **55**, 3807-3812.
18. B. B. Sauer and N. V. Dipaolo, *Journal of Colloid and Interface Science*, 1991, **144**, 527-537.
19. M. Tagawa, K. Gotoh, A. Yasukawa and M. Ikuta, *Colloid and Polymer Science*, 1990, **268**, 589-594.
20. L. Elias, F. Fenouillot, J. C. Majeste and P. Cassagnau, *Polymer*, 2007, **48**, 6029-6040.
21. M. Yousfi, S. Livi, A. Dumas, J. Crépin-Leblond, M. Greenhill-Hooper and J. Duchet-Rumeau, *Journal of Applied Polymer Science*, 2014, In press.
22. m. Yousfi, S. Livi and J. Duchet-Rumeau, *Chemical Engineering Journal*, 2014, **255**, 513-524.
23. S. S. Ray and M. Bousmina, *Macromolecular Rapid Communications*, 2005, **26**, 450-455.
24. F. Fenouillot, P. Cassagnau and J. C. Majeste, *Polymer*, 2009, **50**, 1333-1350.
25. S. C. Wong and Y. W. Mai, *Polymer*, 2000, **41**, 5471-5483.
26. A. N. Wilkinson, L. Laugel, M. L. Clemens, V. M. Harding and M. Marin, *Polymer*, 1999, **40**, 4971-4975.
27. G. Filippone, A. Causa, M. S. de Luna, L. Sanguigno and D. Acierno, *Soft Matter*, 2014, **10**, 3183-3191.
28. Z. Yang, Z. Zhang, Y. Tao and K. Mai, *European Polymer Journal*, 2008, **44**, 3754-3763.
29. M.-L. Xue, Y.-L. Yu and H. H. Chuah, *Journal of Macromolecular Science Part B-Physics*, 2007, **46**, 603-615.
30. M. Psarski, M. Pracella and A. Galeski, *Polymer*, 2000, **41**, 4923-4932.
31. A. Lahor, M. Nithitanakul and B. P. Grady, *European Polymer Journal*, 2004, **40**, 2409-2420.
32. B. W. Chieng, N. A. Ibrahim and W. M. Z. W. Yunus, *Express Polymer Letters*, 2010, **4**, 404-414.
33. L. T. Vo and E. P. Giannelis, *Macromolecules*, 2007, **40**, 8271-8276.
34. Kusmono, Z. A. M. Ishak, W. S. Chow, T. Takeichi and Rochmadi, *European Polymer Journal*, 2008, **44**, 1023-1039.
35. F. Laoutid, E. Estrada, R. M. Michell, L. Bonnaud, A. J. Mueller and P. Dubois, *Polymer*, 2013, **54**, 3982-3993.